Soliton Transmission Capacity of Vertical Cavity Surface Emitting Lasers (VCSELs) Degradation under Thermal Irradiated Fields

Abd El-Naser A. Mohamed[1], Nabil A. Ayad[2], Ahmed Nabih Zaki Rashed[1*] and Hazem M. El-Hageen[1, 2]

[1] Electronics and Electrical Communication Engineering Department,
Faculty Electronic Engineering, Menouf, 32951, Egypt
[2]Atomic Energy Authority, P.O. Box 29, Naser City, Cairo, Egypt
[*]E-mail: ahmed_733@yahoo.com

***Abstract*— This paper has presented the performance of the VCSELs in thermo-irradiated has been modeled, investigated and deeply parametrically analyzed over wide range of the affecting parameters. As well as we have processed soliton transmission capacity of VCSELs based different materials (silica-doped, aluminum gallium arsenide (AlGaAs), and polymer) in thermo-irradiated field effects. Both the ambient temperature and irradiation dose as well as the spectral wavelength possess serve reduction effects on the transmission characteristics (dispersion, and bandwidth) and consequently the transmitted bit rates and products. Useful semi-emperical relations have been cast. Thermo-irradiated penalties were computed and fitted as nonlinear relationships of useful impact in the design model for the device. Analysis of laser characteristics after irradiation showed that the main effect of radiation damage is an increase in bulk recombination that increases loss within the laser cavity. The device performance degradation is proportional to the fluence. The fluence rate is also relevant for degradation in electron irradiation. Low fluence rate leads to larger degradation compared to those associated with high fluence rate resulting from heat impact in bulk. The radiation damage of neutron is larger than irradiation damage of electron, which is caused by the difference in mass and the possibility of nuclear collision for the formation of lattice defects.**

***Keywords*—** VCSELs, Radiation Hardness Assurance, Reliability, Soliton Transmission and Neutrons Irradiation

I. INTRODUCTION

Many advances have been made in laser diodes that have extended the wavelength range over which semiconductor lasers can be used, and also reduced the threshold current required for operation. Key technical advances include the use of thin heterostructures that allow efficient carrier injection over dimensions of 0.1 to 0.2 μm [1], special means of confining carriers within the laser cavity (including interspersed oxide or semiconductor layers), strained layers that reduce losses due to Auger recombination, and small, precise lateral dimensions that provide quantum wells to limit the number of allowable states within the cavity [2].

The oldest material system is AlGaAs-GaAs, used for wavelengths between 0.65 and 0.85 μm. Alloys of AlGaAs are lattice matched with GaAs to about 0.1 %, allowing a wide range of compositions to be used. The second material system is InGaAsP-InP. This combination also allows good lattice matching for various compositional variations [3], and is widely used for wavelengths between 1.1 and 1.6 μm [4]. Close lattice matching is not possible for the wavelength "gap" between 0.85 μm and 1.1 μm. Lasers within that region are made with InGaAs-GaAs, where there is a large amount of lattice mismatch (up to 3 %). Thus, lasers fabricated with this material contain strained layers that must be restricted in thickness in order to avoid lattice defects that would degrade efficiency and reliability. Strained layers can be made with dimensions up to approximately 100 μm [5].

In the present study, we have investigated deeply the performance characteristics of high speed laser diodes such as vertical cavity surface emitting lasers (VCSELs) under thermal irradiated operating conditions over wide range of the affecting parameters. As well as a considerable amount of hard radiation effects studies on individual optoelectronic devices exposed to a variety of radiation conditions is deeply investigated, only little information is available on the radiation tolerance at high total dose and under neutron radiation.

II. SCHEMATIC DIAGRAM OF AlGaAs LASER

As shown in Fig. 1, a simplified diagram of an advanced laser diode (the top and bottom electrical contacts are not shown). The structure includes double-heterojunctions that allow carrier injection over very short distances, and lateral confinement using an oxide layer to restrict carrier injection from the top contact. For this material, the difference in refractive index between the GaAs and AlGaAs regions is sufficient to confine photons to the active region, but some lasers add additional layers that surround the active region for better optical confinement. Several methods can be used for lateral confinement, including ridge structures [6].

Proton displacement damage has been studied in only a few types of laser diodes [7] and little information is available on damage in more advanced devices [8]. The

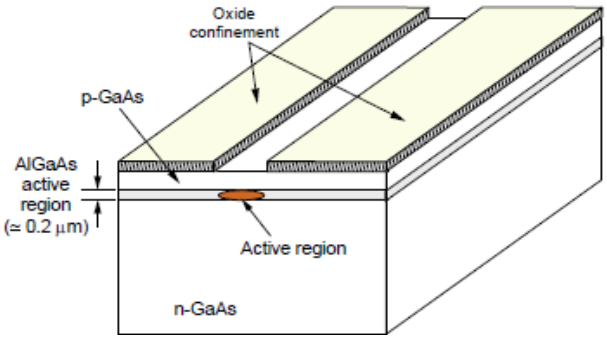

Fig. 1. Diagram of an oxide-confined AlGaAs laser

lasers represent a broad range of current laser technologies. One of the devices is a vertical cavity surface-emitting laser that provides light output from the top surface, and uses a distributed Bragg reflector in combination with lateral oxide confinement in order to obtain high efficiency and low threshold current [9].

III. BASIC MODEL AND ANALYSIS

The degradation of junction diode performance is known to be caused by a decrease in both the minority carrier lifetime and generation lifetime. The decrease of these lifetimes can be related to the total dose φ by the definition of a damage coefficient k:

$$\frac{1}{t_p} = \frac{1}{t_{p0}} + k_p \varphi \quad , \tag{1}$$

$$\frac{1}{t_g} = \frac{1}{t_{g0}} + k_g \varphi \quad , \tag{2}$$

Where φ, k_p , k_g, t_{p0} and t_{g0} are irradiation fluence in n/cm^2, the damage coefficient of minority carrier lifetime, damage coefficient of generation lifetime, initial minority carrier lifetime and initial generation carrier lifetime, respectively. the t_p and t_g depend on the total dose and other parameters are independent of the total dose. When high energy radiation falls on a semiconductor device, energy is deposited in the semiconductor via two mechanisms; atomic displacement or ionization [10]. The relative importance of these mechanisms in a semiconductor depends on the type of radiation and the nature of the device. The electrical resistance of semiconducting metals is very much more sensitive to radiation than that of typical metals because the radiation-induced defects may markedly alter the number of electrons available for conduction. Point defects (initially produced) can be produced by electron or gamma irradiation. It can be expressed as a single displaced atom and its associated vacancy called Frankel Defect. The interaction is simply described by the number of defects/cm^3 created, which is given by [11]:

$$N_t = \varphi \; a_d \; N_0 \quad , \tag{3}$$

Where a_d is the displacement cross-section in cm^2, and N_0 is the number of lattice atoms/cm^3. The point defects result in the introduction of allowed energy states within the forbidden gap of the semiconductor. This energy states lead to the following: (a) Carrier removal is the majority carrier density is reduced by the radiation fluence, (b) Mobility degradation is the mobility was found to decrease with increasing the radiation fluence, (c) Conductivity modulation since the carrier concentration and mobility both decrease with radiation, then the conductivity will also decrease, and (d) Minority carriers lifetime can be defined as the degradation rate in minority carrier lifetime and can be expressed as:

$$\frac{d\tau}{d\varphi} = K_\tau \tag{4}$$

Where K_τ is the carrier lifetime damage constant. The minority carrier lifetime τ will be reduced by [12]:

$$\frac{1}{\tau} = \frac{1}{\tau_0} + \sum_i \nu_{th} \, \sigma_i \, n_i \quad , \tag{5}$$

Where τ_0 is the pre-irradiation minority carrier lifetime, υ_{th} is the average thermal velocity of the minority carriers, n_i and σ_i are the density and capture cross section, respectively, of the recombination centers of a given type i, and the sum extends over the different types of radiation induced defects. As long as there is no significant overlap of the defect regions produced by the individual incident particles [13], the initial defect density will be proportional to the particle fluence φ as the following expression:

$$n_i = c_i \, \varphi \, I \quad , \tag{6}$$

Where I is the light current output, and the coefficient c_i stands for the density of particular defects per unit fluence. Defining a damage constant K_τ is:

$$K_\tau = \nu_{th} \sum_i c_i \, \sigma_i \quad , \tag{7}$$

Where K_τ is sensitive to many factors such as material, type of radiation, particle energy, flux, device temperature and electrical bias conditions. The ratio τ_0/τ of the minority carrier lifetime before and after the irradiation can be related to the relative light output after irradiation assuming that the total current density in the junction is dominated by diffusion currents as the following expression [15]:

$$\left(\frac{I_0}{I}\right)^{2/3} = \frac{\tau_0}{\tau} \quad , \tag{8}$$

Where I_0 is pre-irradiation light current output. Thus, the parameter $k = \tau_0 K_\tau$ can be calculated from the relative light output (RLO) of the devices after the irradiation with a total particle fluence φ;

$$\left(\frac{1}{RLO}\right)^{2/3} = \left(\frac{I_0}{I}\right)^{2/3} = 1 + k\varphi \quad , \tag{9}$$

The power forward current curves of different types of VCSEL devices were given in [16], with remarkable nonlinearly while in [17] it depicted in linear fashion. Based on the data of [18], the following nonlinear thermal relations for the set of the selected device were carried out:

$$P(I,T) = p_0 + p_1 I + p_2 I^2 \, , \quad \text{mWatt} \tag{10}$$

Where the set of parameters {p_0, p_1, and p_2} are polynomial functions of ambient temperature T.

$$p_0 = 0.73 - 0.00169 \; T + 0.000345 \; T^2 \, , \tag{11}$$

$$p_1 = 2.5 - 0.0072 \; T + 0.0002 \; T^2 \, , \tag{12}$$

$$p_2 = -7.3 - 0.002 \; T + 0.000065 \; T^2 \, , \tag{13}$$

The power of VCSEL under the effects of irradiation can be expressed in the following formula:

$$P(I,T,\varphi) = P(I,T) \, F_p(\varphi) \quad , \tag{14}$$

Where $F_p(\varphi)$ is a function of the irradiation fluence φ, can be expressed as follows:

$$F_p(\varphi) = 1 + \alpha_1 \varphi + \alpha_2 \varphi^2 \quad , \tag{15}$$

Where the set of the coefficients of α_1=0.0005, α_2=-0.001. The standard single mode fiber link within VCSEL based silica doped material which the investigation of the spectral variations of the waveguide refractive-index, n require empirical equation under the form [19]:

$$n^2 = 1 + \frac{A_1 \lambda^2}{\lambda^2 - A_2^2} + \frac{A_3 \lambda^2}{\lambda^2 - A_4^2} + \frac{A_5 \lambda^2}{\lambda^2 - A_6^2} \tag{16}$$

The empirical equation coefficients as a function of temperature and Germania mole fraction, x as:
A_{1S}=0.691663+0.1107001x,
A_{2S}=(0.0684043+0.000568306x)^2(T/T_0)^2,
A_{3S}=0.4079426+0.31021588x,
A_{4S}= (0.1162414+0.03772465x)^2(T/T_0)^2, A_{5S}=0.8974749-0.043311091x, A_{6S}=(9.896161+1.94577x)^2. Where T is ambient temperature in K, and T_0 is the room temperature and is considered as 300 K. First and second differentiation of empirical equation w. r. t operating wavelength λ as in

Ref. [20] for both silica-doped and polymer materials. For the plastic fiber material, the coefficients of the Sellmeier equation and refractive-index variation with ambient temperature are given as: A_{1P}= 0.4963, A_{2P}= 0.6965 (T/T_0), A_{3P}= 0.3223, A_{4P}= 0.718 (T/T_0), A_{5P}= 0.1174, and A_{6P}= 9.237. For Aluminum Gallium Arsenide (AlGaAs), the set of parameters required to characterize the temperature and operating wavelength dependence of the refractive-index, where empirical equation is under the form of [20]:

$$n^2 = B_1 + \frac{B_2}{\lambda^2 - B_3} - B_4\lambda^2, \quad (17)$$

The set of parameters is recast and dimensionally adjusted as: B_1=10.906, B_2=0.975, B_3=0.3464499 (T/T_0), B_4=0.002467 (0.93721+2.0857x10^{-4} T). Where T is the ambient temperature in K, and T_0 is the room temperature (300 K). We differentiate of previous empirical equation w. r. t λ as mentioned in Ref. [19].

The idea of soliton transmission is to guide the nonlinearity to the desired direction and use it for our benefit. When soliton pulses are used as an information carrier, the effects of dispersion and nonlinearity balance each other and thus don't degrade the signal quality with the propagation distance. In addition, the unique features of soliton transmission can help to solve the problems of data transmission, because the soliton data looks essentially the same at different distances along the transmission, the soliton type of transmission is especially attractive for all-optical data networking. Moreover, because of the high quality of the pulses and return-to-zero (RZ) nature of the data the soliton data is suitable for all-optical processing. In any infinitesimal segment of fiber, dispersion on one hand and non linearity of the refractive-index on the other hand produce infinitesimal modulation angles which exactly compensate reciprocally. In the sense that their sum is an irrelevant constant phase shift. Under such conditions the pulse shape is the same everywhere. The soliton waveform be used with a peak power under the effects of irradiation fluence, temperature and threshold current [21]:

$$P(I,T,\varphi) = \frac{\lambda_s^3 D_t A_{eff}}{12.7\, c\, n_{nl}\, \Delta\tau^2}, \quad (18)$$

Where n_{nl} is the nonlinear Kerr coefficient, 2.6 x 10^{-20} m^2/Watt, λ is the operating signal wavelength in μm, A_{eff} is the effective area of the plastic fiber in μm^2, c is the velocity of light (3x10^8 m/sec). The total bandwidth is based on the total chromatic dispersion for silica-doped and AlGaAs based VCSEL is given by:

$$D_t = D_m + D_w \quad (19)$$

Where D_m is the material dispersion and D_w is the waveguide dispersion as mentioned in Ref. [22]. Also the total dispersion coefficient in nsec/m^2 of the polymer material based VCSEL is given by:

$$D_t = \left(M_{md} + P\right), \quad (20)$$

In which M_{md} is the material dispersion and P is the profile dispersion as listed in Ref. [22]. Then the total pulse broadening from Eq. 19 can be expressed as the following:

$$\Delta\tau = \sqrt{\frac{\lambda^3 D_t A_{eff}}{12.7\, P(I,T,\varphi)\, n_{nl}\, c}}, \quad (21)$$

The bandwidth for standard single mode fibers for both materials based VCSEL device is given by [23]:

$$B.W_{sig.} = \frac{0.44}{\Delta\tau \,.\, L}, \quad (22)$$

Then the soliton transmission bit rate is given by [23]:

$$B_{RS} = \frac{1}{10\Delta\tau} = \frac{0.1}{\Delta\tau}, \quad (23)$$

Where L is the transmission VCSEL laser diode reach.

IV. SIMULATION RESULTS AND DISCUSSIONS

We have investigated transmission bit rates and bandwidth transmission reach products of VCSEL devices under the effects of the thermo-Irradiated environments under the assumed set of the operating parameters and ranges as: irradiation fluence $2x10^{14} \le \varphi \le 5x10^{14}$ n/cm^2, Ambient temperature 290 ≤ T, K ≤ 330, applied drive current 10 ≤ I, mA ≤ 50, room temperature T_0=300 K, effective area A_{eff}=85 μm^2, index exponent α=2, spectral linewidth of the optical source Δλ= 0.2 nm, signal power Pso=2 mWatt, germanium dopant ratio x=0.3, Operating optical signal wavelength 0.65 ≤ λ_s, μm ≤ 1.65, silica relative refractive index difference Δn_s= 0.003, AlGaAs relative refractive index difference Δn_{AlGaAs}=0.003, polymer relative refractive index difference Δn_p= 0.03, initial device gain, g_0=8.5x10^6, thermal rate R_{th}=0.85, transmission laser diode reach L=50 m, N_0=1.3x10^6. It is necessary to stress that the major generator of features is the irradiation fluence due to the damage which causes dislocations; and radiation-induced defects is the band gap. Based on the above model and the series of the operating parameters variations of the set of five causes {3-dB signal transmitted bandwidth $f_{3\text{-}dB}$, device transmission bit rates and products} against the variations of a set of effects {irradiation fluence φ, ambient temperature T, applied threshold current I} are displayed in the series of Figs. (2-14):

i) As shown in Fig. 2 has assured that as the drive current of the VCSEL diode increases, this leads to increase of output device power. We have observed that after two neutrons fluences, the output device power is decreased compared to that its value before irradiation.

ii) As shown in the series of Figs. (3-8), as ambient temperature increases, these results in decreasing in soliton transmission bit rates for different materials based VCSEL devices after or before irradiation. As well as we have demonstrated after two neutrons fluences, the soliton transmission bit rates for different based VCSEL devices degraded and decreased fastly. This illustrates the harmful effects of the neutrons irradiation on the performance characteristics of these devices, especially for transmission bit rates.

iii) As shown in the series of Figs. (9-14), as ambient temperature increases, these results in decreasing in transmitted signal bandwidth for different materials based VCSEL devices after or before irradiation. As well as we have indicated after two neutrons fluences, the transmitted signal bandwidth for different based VCSEL devices degraded and decreased fastly. This illustrates the harmful effects of the neutrons irradiation on the performance characteristics of these devices, especially for transmitted signal bandwidths.

iv) As shown in the series of Figs. (2-14), we have assured that as the drive current increases, this leads to increase of output device power, and then to increase both transmission bit rates and transmitted signal bandwidths.

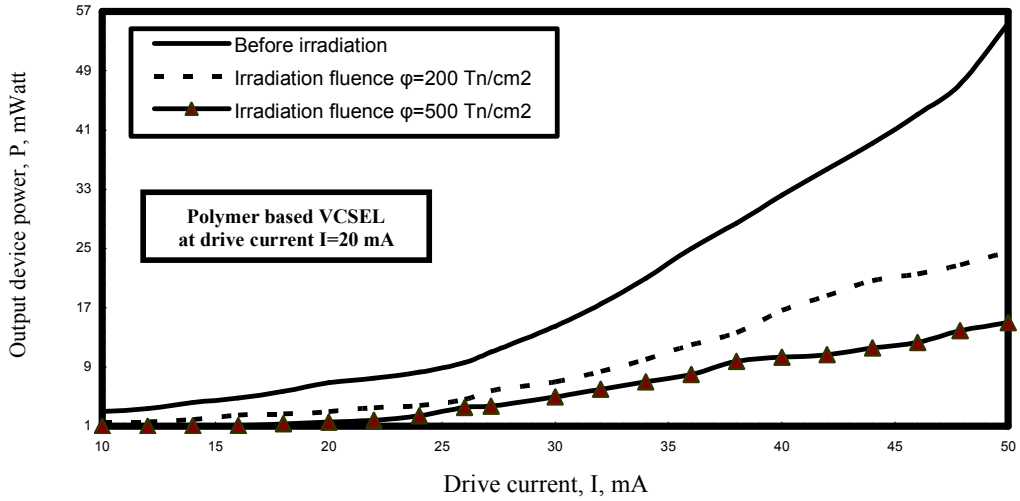

Fig. 2. Variations of the output power against drive current for a typical VCSEL after two neutrons fluences at the assumed set of parameters.

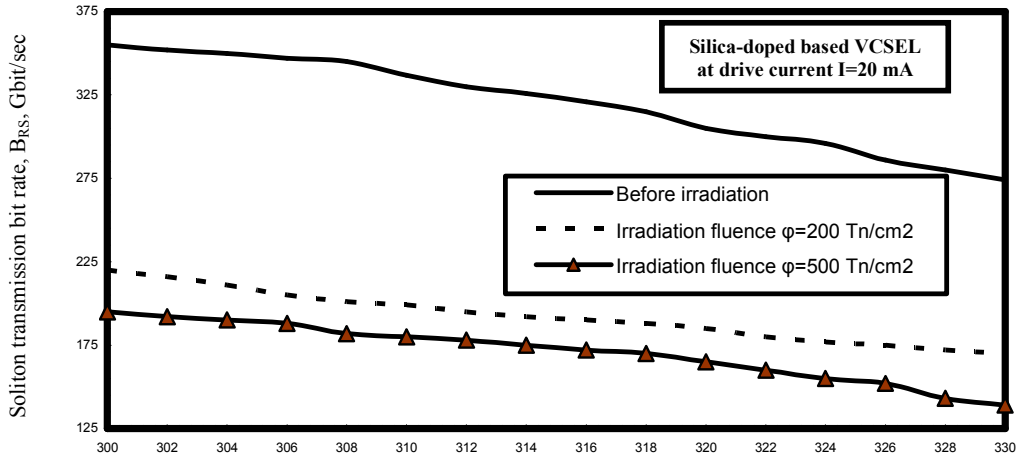

Fig. 3. Variations of the soliton transmission bit rate against ambient temperature after two neutrons fluences at the assumed set of parameters.

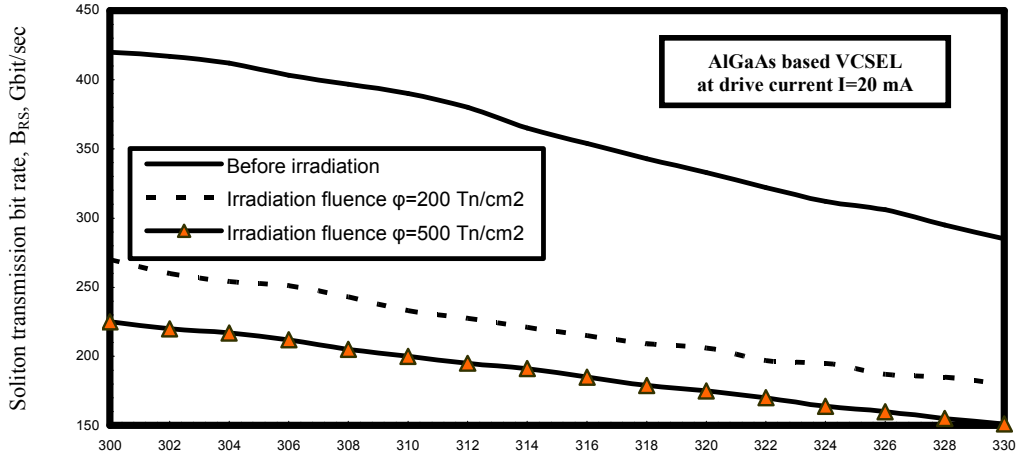

Fig. 4. Variations of the soliton transmission bit rate against ambient temperature after two neutrons fluences at the assumed set of parameters.

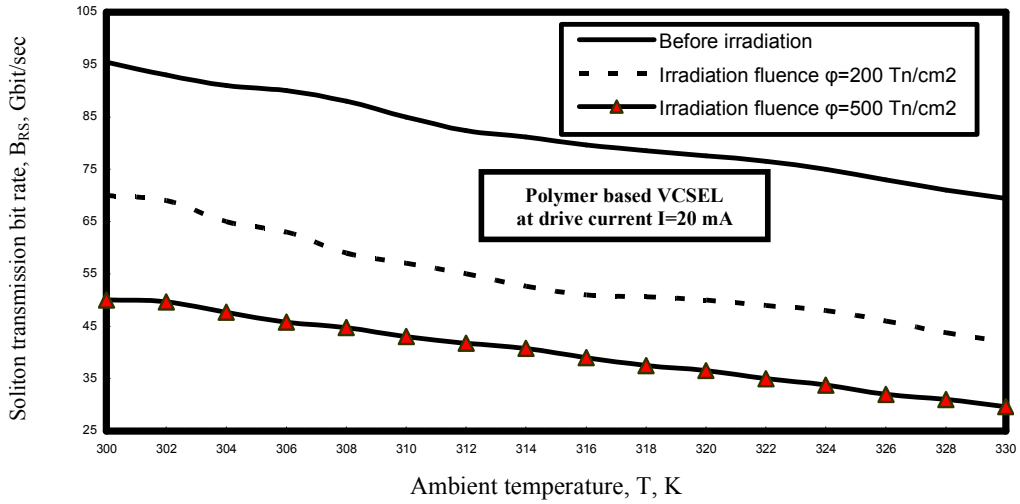

Fig. 5. Variations of the soliton transmission bit rate against ambient temperature after two neutrons fluences at the assumed set of parameters.

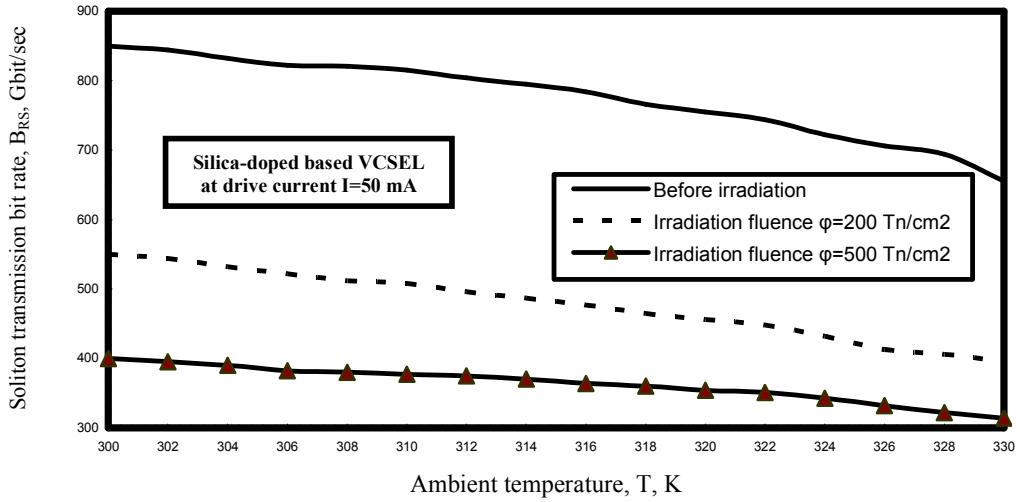

Fig. 6. Variations of the soliton transmission bit rate against ambient temperature after two neutrons fluences at the assumed set of parameters.

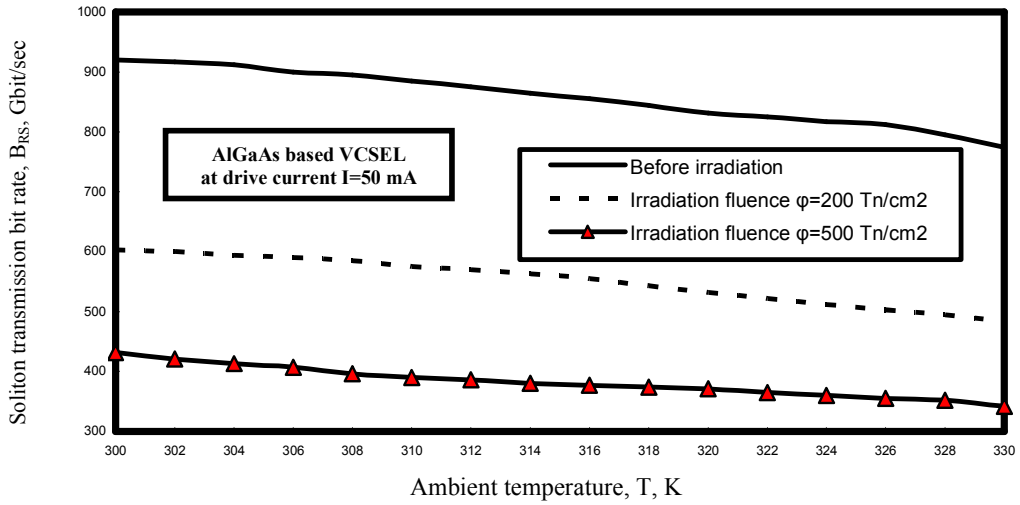

Fig. 7. Variations of the soliton transmission bit rate against ambient temperature after two neutrons fluences at the assumed set of parameters.

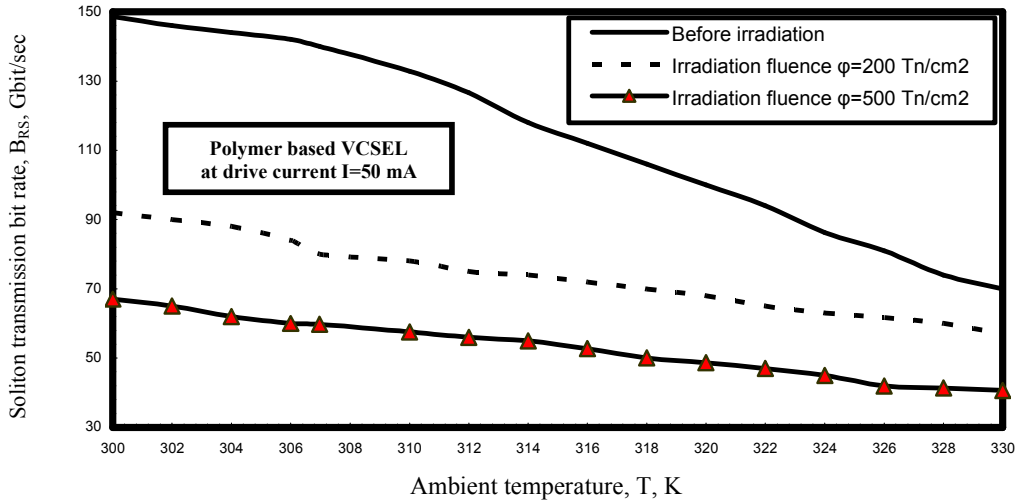

Fig. 8. Variations of the soliton transmission bit rate against ambient temperature after two neutrons fluences at the assumed set of parameters.

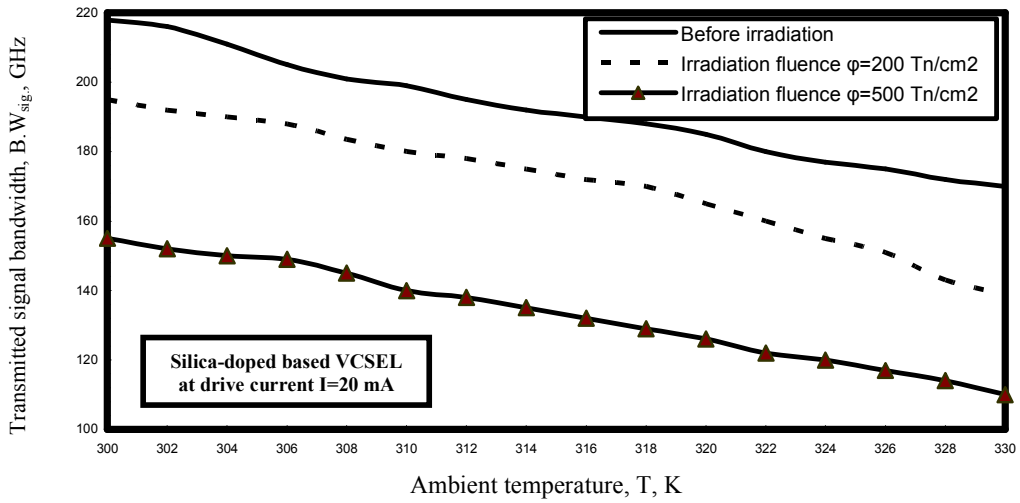

Fig. 9. Variations of the transmitted signal bandwidth against ambient temperature after two neutrons fluences at the assumed set of parameters.

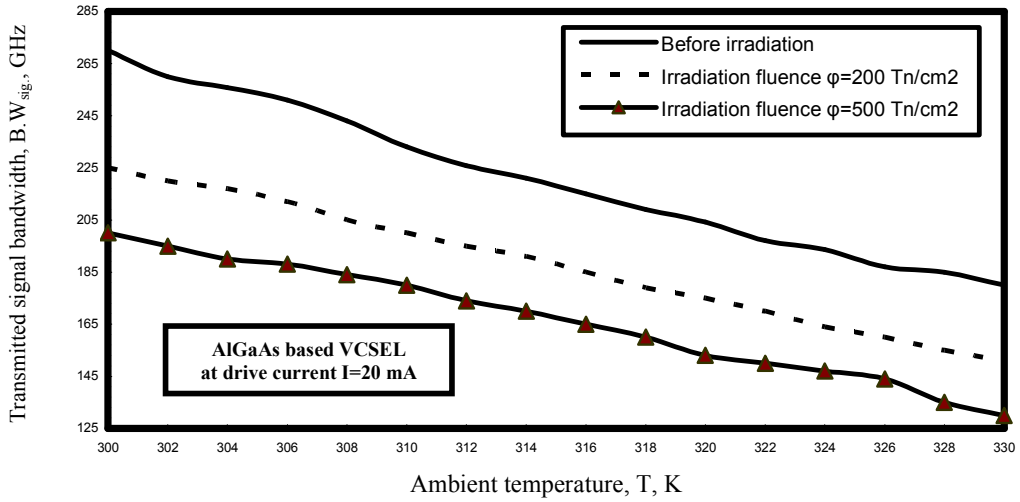

Fig. 10. Variations of the transmitted signal bandwidth against ambient temperature after two neutrons fluences at the assumed set of parameters.

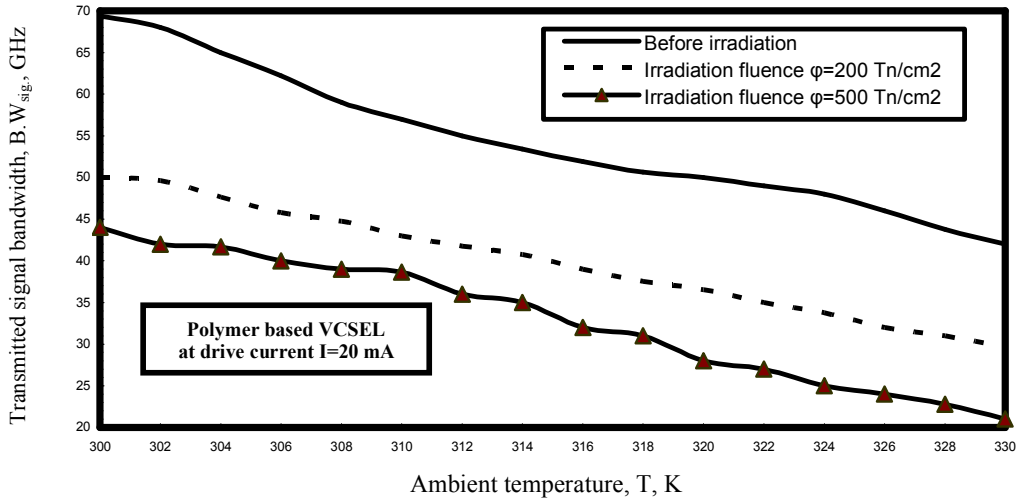

Fig. 11. Variations of the transmitted signal bandwidth against ambient temperature after two neutrons fluences at the assumed set of parameters.

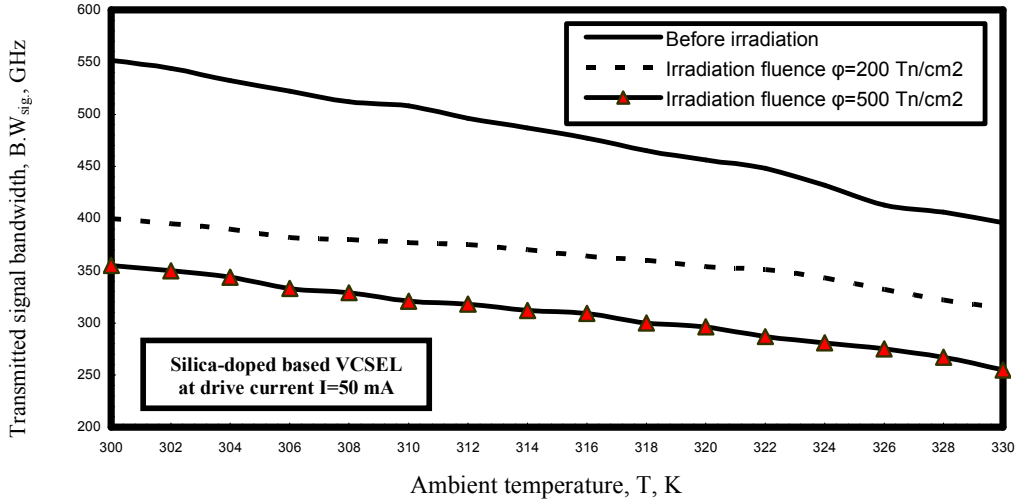

Fig. 12. Variations of the transmitted signal bandwidth against ambient temperature after two neutrons fluences at the assumed set of parameters.

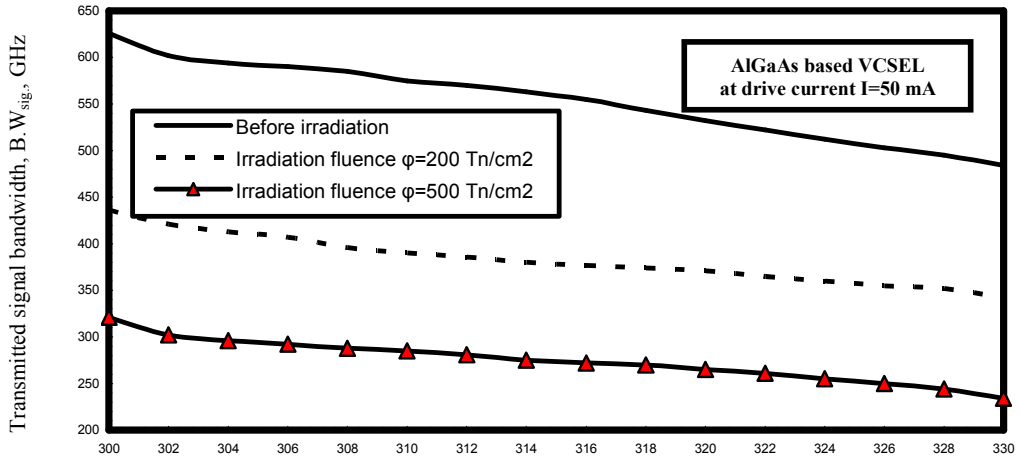

Fig. 13. Variations of the transmitted signal bandwidth against ambient temperature after two neutrons fluences at the assumed set of parameters.

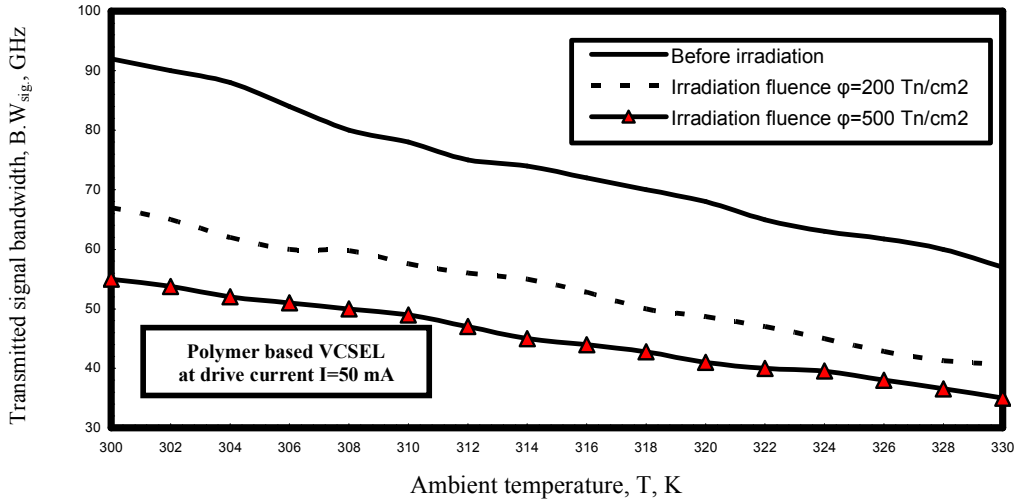

Fig. 14. Variations of the transmitted signal bandwidth against ambient temperature after two neutrons fluences at the assumed set of parameters.

V. CONCLUSIONS

In a summary, we have deeply investigated the low performance characteristics of VCSEL devices under thermal irradiation fields over wide range of the affecting parameters. It is theoretically found that the increased drive current of VCSEL devices this results in the increased output device power. As well as we have observed that the output device power is decreased dramatically after two neutrons fluences. It is also indicated that the increased both ambient temperature and neutrons irradiation fluences this leads to the decreased of both soliton transmission bit rates and transmitted signal bandwidths for different materials based VCSEL devices. Therefore we have demonstrated the harmful effects of both ambient temperature and neutrons irradiation fluences over different materials based VCSEL devices that affect negatively on the performance characteristics of the VCSEL devices.

REFERENCES

[1] C. A. Ramos, R. DE Oliveria, A. T. Marques, and O. Frazao, "Measurement of Dynamic Strain Using an Optic Fiber System in Adaptive Composite Laminates With an Integrated Piezoelectric Sensor/Actuator," Optica Applicata, Vol. XLI, No. 1, pp. 79-87, 2011.

[2] R. Kasztelanic, "Surface Plasmon Resonance Sensors Novel Architecture and Improvements," Optica Applicata, Vol. XLI, No. 1, pp. 145-155, 2011.

[3] M. Y. Aldouri, and H. A. Fadhil, "Bit Error Rate (BER) Performance of Return to Zero and Non Return to Zero Data Signals Optical Code Division Multiple Access (OCDMA) System Based on AND Detection Scheme in Fiber to The Home (FTTH) Networks," Optica Applicata, Vol. XLI, No. 1, pp. 207-216, 2011.

[4] B. Abbas, and M. A. Khalil, "Absorption Characteristics of Disperse Blue Dioxane Solutions," Optica Applicata, Vol. XLI, No. 1, pp. 173-181, 2011.

[5] Sh. M. Eladl, "Modeling of Photons Trapping Effect on the Performance of HPT-LED Optoelectronic Integrated Device (OEID)," Semiconductor Physics, Quantum Electronics & Optoelectronics Journal, Vol. 12, No. 3, pp. 255-259, 2009.

[6] M. V. Raghavendra, and P. L. H. Vara Prasad, "Estimation of Optical Link Length for Multi Haul Applications," International Journal of Engineering Science and Technology, Vol. 2, No. 6, pp. 1485-1491, 2010.

[7] S. W. Cheong, and K. L. Woon, "Modeling of Light Extraction Efficiency of Scattering Thin Film Using Mie Scattering," Optica Applicata, Vol. XLI, No. 1, pp. 217-223, 2011.

[8] M. Dehghan, and E. Darabi, "Investigation and analysis of time response in Geiger mode avalanche photodiode," Optica Applicata, Vol. XL, No. 2, pp. 471-479, 2010.

[9] S. M. Razzak, and Y. Namihira, "Theoretical design of a large effective mode area microstructure optical fiber ," Optica Applicata, Vol. XL, No. 3, pp. 677-683, 2010.

[10] Fu Xiansong, and Ge Tao, and De Maolin, "A study on temperature characteristics of green silicon photodetector," Optica Applicata, Vol. XL, No. 4, pp. 935-941, 2010.

[11] S. Christopoulos, G. von H¨ogersthal, A. Grundy, P. G. Lagoudakis, A. V. Kavokin, J. J. Baumberg,G.Christmann, R. Butt´e, E. Feltin, J.-F. Carlin, and N. Grandjean, "Room Temperature Polariton Lasing in Semiconductor Microcavities," Phys. Rev. Lett., Vol. 98, pp. 1–4, 2007.

[12] S.-H. Park, J. Kim, H. Jeon, T. Sakong, S.-N. Lee, S. Chae, Y. Park, C.-H. Jeong, G.-Y. Yeom, and Y.-H. Cho, "Room Temperature GaN Vrtical Cavity Surface Emitting Laser Operation in an Extended Cavity Scheme," Appl. Phys. Lett., Vol. 83, pp. 21–23, 2003.

[13] E. Feltin, G. Christmann, J. Dorsaz, A. Castiglia, J.-F. Carlin, R. Butt´e, N. Grandjean, S. Christopoulos, G. Baldassarri, H. von H¨ogersthal, A. J. D. Grundy, P. G. Lagoudakis, and J. J. Baumberg, "Blue Lasing at Room Temperature in an Optically Pumped Lattice Matched AlInN/GaN VCSEL Structure," Electron. Lett., Vol. 43, pp. 924–926, 2007.

[14] J.-T. Chu, T.-C. Lu, H.-H. Yao, C.-C. Kao, W.-D. Liang, J.-Y. Tsai, H.-C. Kuo, and S.-C. Wang, "Room-Temperature Operation of Optically Pumped Blue Violet GaN Based Vertical Cavity Surface Emitting Lasers Fabricated by Laser Lift Off," Jpn. J. Appl. Phys, Vol. 45, pp. 2556–2560, 2006.

[15] J.-T. Chu, T.-C. Lu, M. You, B.-J. Su, C.-C. Kao, H.-C. Kuo, and S.-C. Wang, "Emission Characteristics of Optically Pumped GaN Based Vertical Cavity Surface- Emitting Lasers," Appl. Phys. Lett., Vol. 89, pp. 1–3, 2006.

[16] Abd El-Naser A. Mohammed, Mohamed M. S. El-Halawany, Gaber E. M. El-Abyad and Mohammed S. F. Tabbour "Performance Characteristics of High Speed Laser Diodes Under Thermal Irradiated Operating Conditions," Journal Media and Communication Studies, Vol. 2, No. 5, pp. 127-132, May 2010

[17] C.-C. Kao, T. C. Lu, H. W. Huang, J. T. Chu, Y. C. Peng, H. H. Yao, J. Y. Tsai, T. T. Kao, H. C. Kuo, S. C. Wang, and C. F. Lin, "The Lasing Characteristics of GaN Based Vertical

Cavity Surface Emitting Laser With AlN–GaN and Ta2O5 – SiO2 Distributed Bragg Reflectors," IEEE Photon. Technol. Lett., Vol. 18, No. 7, pp. 877–879, 2006.

[18] E. Petrolati and A. D. Carlo, "The Influence of Mobility Unbalance on GaN Based Vertical Cavity Surface Emitting Lasers," Appl. Phys. Lett., Vol. 92, pp. 15–18, 2008.

[19] Abd El-Naser A. Mohammed, Abd El-Fattah A. Saad, and Ahmed Nabih Zaki Rashed, "Study of the Thermal and Spectral Sensitivities of Organic-Inorganic Fabrication Materials Based Arrayed Waveguide Grating for Passive Optical Network Applications," Journal of Engineering and Technology Research, Vol. 1, No. 5, pp. 81-90, August 2009.

[20] Osama A. Oraby, "Propagation of An Electromagnetic Beams in Nonlinear Dielectric Slab Wave Guides," Minufiya Journal of Electronic Engineering Research, Vol. 16, No. 1, pp. 27-44, 2006.

[21] Abd El-Naser A. Mohammed, Gaber E. S. M. El-Abyad, Abd El-Fattah A. Saad, and Ahmed Nabih Zaki Rashed, "High Transmission Bit Rate of A thermal Arrayed Waveguide Grating (AWG) Module in Passive Optical Networks," IJCSIS International Journal of Computer Science and Information Security, Vol. 1, No. 1, pp. 13-22, May 2009.

[22] Abd El-Naser A. Mohammed, Abd El-Fattah A. Saad, and Ahmed Nabih Zaki Rashed,"Thermal Sensitivity Coefficients of the Fabrication Materials Based A thermal Arrayed Waveguide Grating (AWG) in Wide Area Dense Wavelength Division Multiplexing Optical Networks," International Journal of Engineering and Technology (IJET), Vol. 1, No. 2, pp. 131-139, June 2009.

[23] Abd El-Naser A. Mohammed, Gaber E. S. M. El-Abyad, Abd El-Fattah A. Saad, and Ahmed Nabih Zaki Rashed, "Low Loss A thermal Arrayed Waveguide Grating (AWG) Module for Passive and Active Optical Network Applications," International Journal of Communication Networks and Information Security (IJCNIS), Vol. 1, No. 2, pp. 27-34, Aug. 2009.

Dr. Ahmed Nabih Zaki Rashed was born in Menouf city, Menoufia State, Egypt country in 23 July, 1976. Received the B.Sc., M.Sc., and Ph.D. academic scientific degrees in the Electronics and Electrical Communications Engineering Department from Faculty of Electronic Engineering, Menoufia University in 1999, 2005, and 2010 respectively. Currently, his job carrier is a scientific lecturer in Electronics and Electrical Communications Engineering Department, Faculty of Electronic Engineering, Menoufia university, Menouf, the postal Menouf city code: 32951, Egypt country. His scientific master science thesis has focused on polymer fibers in optical access communication systems. Moreover his scientific Ph. D. thesis has focused on recent applications in linear or nonlinear passive or active in optical networks. His interesting research mainly focuses on transmission capacity, a data rate product and long transmission distances of passive and active optical communication networks, wireless communication, radio over fiber communication systems, and optical network security and management. He has published many high scientific research papers in high quality and technical international journals in the field of advanced communication systems, optoelectronic devices, and passive optical access communication networks. His areas of interest and experience in optical communication systems, advanced optical communication networks, wireless optical access networks, analog communication systems, optical filters and Sensors, digital communication systems, optoelectronics devices, and advanced material science, network management systems, multimedia data base, network security, encryption and optical access computing systems. He is a reviewer member in high impact scientific research international journals in the field of Electronics, Electrical communication and advanced optical communication systems and networks. He is also distinguish member in the editorial board of high academic scientific research International Journals in the field of electronics, information systems, optoelectronics, communication networks, wireless optical communication systems, and communication technologies. His personal electronic mail ID is (ahmed_733@yahoo.com).